

Endogenous p53 Protein Generated from Wild-Type Alternatively Spliced p53 RNA in Mouse Epidermal Cells

MOLLY F. KULESZ-MARTIN,* BARBARA LISAFELD, HUA HUANG, NICHOLAS D. KISIEL,
AND LAURA LEE

Department of Experimental Therapeutics, Roswell Park Cancer Institute, Buffalo, New York 14263

Received 13 August 1993/Returned for modification 21 October 1993/Accepted 24 November 1993

We previously demonstrated that a wild-type alternatively spliced p53 (p53as) RNA exists in mouse cultured cells and normal mouse tissues at approximately 25 to 33% of the level of the major p53 RNA form. The alternative RNA transcript is 96 nucleotides longer than the major transcript as a result of alternative splicing of intron 10 sequences. The protein expected to be generated from the p53as transcript is 9 amino acids shorter than the major p53 protein and has 17 different amino acids at the carboxyl terminus. We report here that p53as protein exists in nontransformed and malignant epidermal cells and is localized to the nucleus. In addition, p53as protein is preferentially expressed during the G₂ phase of the cell cycle and in cells with greater than G₂ DNA content compared with the major p53 protein, which is preferentially expressed in G₁. The p53as immunoreactivity is elevated and shifted to the G₁ phase of the cell cycle following actinomycin D treatment of nontransformed cells but not malignant cells. In view of the dimerization and tetramerization of p53 protein which may be necessary for its DNA binding and transcriptional activation activities, the presence of p53as protein in cells has important implications for understanding the physiological function(s) of the p53 gene.

The tumor suppressor gene p53 is the most frequently altered gene in human cancers, mutations or deletions of p53 being detected in over half of all tumors (44). Introduction of wild-type (wt) p53 into a variety of transformed or tumor cells arrests their growth (7, 11) or induces programmed cell death (apoptosis) (51, 52). These observations suggest that defects in the p53 gene are acquired during cancer development along multiple initiation and promoting pathways and that cells with various accumulated defects are sensitive to tumor growth arrest by wt p53 protein, making this gene of widespread interest.

Human and mouse p53 share an 81% identity at the protein level, with a highly acidic N terminus, a basic C terminus, and a central region containing uncharged amino acids (40). The studies of the p53 gene in cells, tissues, or cell-free systems have led to the assignment of certain conserved functional domains, as summarized by Vogelstein and Kinzler (reference 45 and references therein) (Fig. 1). Heat shock protein binding and transcriptional activation domains are found near the N terminus, while nuclear localization signals and regions required for heat shock protein binding (35) are located near the C terminus. Residues important for self-association of p53 are present within the 47 C-terminal amino acids (13, 19, 31), including acidic and basic residues important for dimerization and tetramerization, respectively (15, 43). Several monoclonal antibodies to mouse p53 protein are differentially reactive to wt p53 in the normal, tumor-suppressive conformation (PAb246), to denatured wt and mutant p53 (PAb421) (46, 50), or to certain mutant p53 proteins (PAb240) (reference 42 and references therein). There are sites for phosphorylation by casein kinase II (serine 389) (28) and p34^{cdc2} kinase and for covalent linkage of 5.8S rRNA (12). Studies using p53 protein generated *in vitro*, in bacteria, or in baculovirus systems have indicated that p53 probably binds to DNA as a tetramer (3, 41) and activates (10, 47, 53) or represses (39) the transcription of target genes. Mutations in several hot spots within conserved

sequences of the p53 gene result in p53 proteins which are defective in oligomerization, DNA binding, or transcriptional activation.

We have previously reported that wt p53 is abnormally regulated early after malignant conversion in chemically transformed mouse epidermal cells, prior to any coding region mutations (16). In squamous cell carcinomas from two independently initiated cell lineages, wt p53 RNA abundance is increased at the point of malignant conversion. Immunodetectable p53 protein (detected with monoclonal anti-p53 antibodies PAb421 and PAb246) is very low in one carcinoma line and elevated approximately threefold in the other, suggesting that there may be multiple mechanisms of p53 inactivation in chemically transformed epidermal cells. Others have shown that mutations of p53 are absent in papillomas and early squamous cell carcinomas induced by 7,12-dimethylbenz[α]anthracene and 12-O-tetradecanoylphorbol-13-acetate but are present later in promotion in 25 to 50% of squamous cell carcinomas, which tend to possess a metastatic or poorly differentiated phenotype (37). Burns et al. (5) reported that p53 mutations occurred prior to degeneration of squamous cell carcinomas into undifferentiated spindle cell carcinomas. The mutation or altered protein abundance of p53 in malignant epidermal cells corroborates the recent findings of Ro et al. (36) that immunodetectable p53 is elevated in malignant but not benign human epidermal tumors.

During the sequencing of p53 cDNA from the tumor and normal cells of the mouse cloned keratinocyte model, we detected an alternatively spliced p53 mRNA in which 96 nucleotides of the 3' end of intron 10 are inserted between nucleotides 1091 and 1092 of the mouse p53 gene (1 being adenine of the first ATG codon) (17). This p53 variant was first cloned as a mutant p53 cDNA (M-8) from a chemically transformed fibroblast cell line by Wolf et al. (48). Arai et al. (1) reported its sequence, confirming its origin by alternative splicing. It appeared to be specific to this tumor cell lineage because it was undetectable in a nontransformed helper T-cell cDNA library. However, we demonstrated that wt alternatively spliced p53 RNA was expressed in normal cells and tissues at

* Corresponding author. Phone: 716-845-5918. Fax: 716-845-8857.

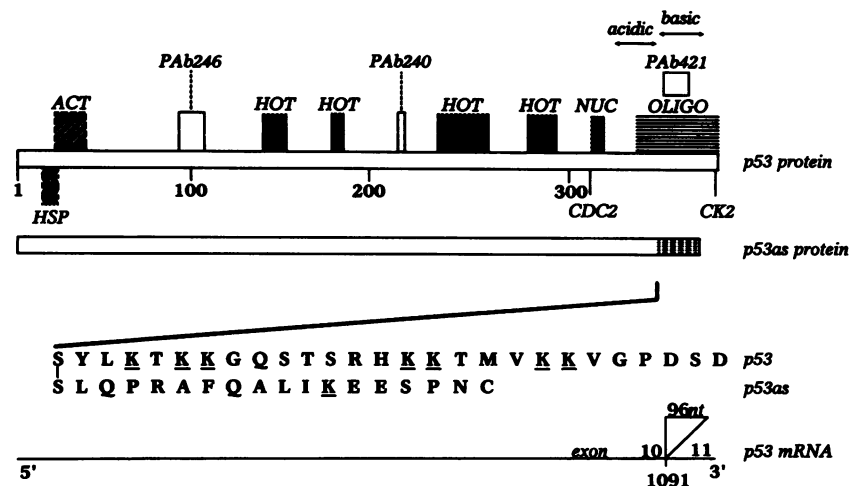


FIG. 1. Domain map of p53 protein showing changes introduced by alternative splicing. Mouse p53 has 390 amino acids; human p53 has 393. Domains (reference 45 and references therein): ACT, transcriptional activation domain; HSP, heat shock protein binding region of mutant p53; HOT, hot spots (highly conserved regions among p53 proteins in which most transforming mutations occur); PAb240, region binding antibody conformation specific for certain mutants, murine amino acids 210 to 214; PAb246, region binding antibody to normal wt conformation, murine amino acids 88 to 109; PAb421, region binding antibody to wt and mutant conformation, amino acids 370 to 378; NUC, nuclear localization signal; CDC2, CDC2 kinase serine phosphorylation site; CK2, casein kinase II serine phosphorylation site, which is also the site of 5.8S rRNA binding; OLIGO, site of p53 self-association. nt, nucleotides. The expected changes in the C-terminal region of protein translated from alternatively spliced wt (17) or mutant (1) p53 mRNA are shown. The segment of intron 10 retained in p53as mRNA is indicated as a triangle between exons. Acidic amino acids (within a predicted alpha helix spanning positions 334 to 356) and basic amino acids (between positions 363 and 386; underlined in the C-terminal peptide sequence at the bottom) are labeled according to Sturzbecher et al. (43). (Figure adapted in part from reference 45 with permission of the author and publisher.)

about 25 to 33% of the level of the major p53 RNA form (17). In addition, it was present at approximately the same ratio in the two independently derived epidermal carcinoma lines which overexpress p53 RNA (noted above) and thus appeared to be coordinately elevated with the major form of p53.

The translation of alternatively spliced p53 results in the substitution of 17 amino acids and in truncation of the regularly spliced form of p53 by 9 amino acids (Fig. 1). The protein translated from the alternatively spliced p53 RNA would lack the serine 389 casein kinase II and RNA binding site, the epitope for PAb421 p53 antibody binding, and the basic oligomerization domain, with the potential for profound effects on p53 oligomerization, DNA binding, and transcriptional activation.

In spite of the evidence for alternative mRNA species from the single p53 gene, to date no wt endogenous variants of p53 protein have been detected. We report here that the alternatively spliced wt p53 protein (which we designated p53as, for alternative splice) exists in normal and tumor cells of a mouse epidermal cell transformation model and is differentially expressed during the cell cycle relative to the major p53 form. The presence of this physiological form of p53 protein in cells has important implications for normal p53 function and p53 inactivation in malignancy.

MATERIALS AND METHODS

Cells. Strain 291 was derived from neonatal BALB/cROS mouse epidermis (West Seneca Laboratory, Roswell Park Cancer Institute [RPCI]) and is normal with respect to differentiation and morphology in vitro and in vivo (22, 26, 38). The cells were grown in Eagle's minimum essential medium with Earle's salts without CaCl_2 (GIBCO, Grand Island, N.Y.), supplemented with 5% (vol/vol) fetal calf serum treated with Chelex-100 resin (Bio-Rad, Rockville Center, N.Y.) to reduce

Ca^{2+} concentration, nonessential amino acids, 10% (vol/vol) mouse dermal fibroblast conditioned medium, 10 ng of epidermal growth factor (Upstate Biotechnology, Inc., Lake Placid, N.Y.) per ml, 1% (vol/vol) antibiotic-antimycotic (penicillin [100 U/ml], streptomycin sulfate [100 $\mu\text{g}/\text{ml}$], and amphotericin B solution [0.25 $\mu\text{g}/\text{ml}$]; GIBCO), and 0.02 to 0.04 mM Ca^{2+} (designated low- Ca^{2+} [LC] conditions). Tumor cell derivatives of 291 (291.03RAT and 291.05RAT) were isolated from squamous cell carcinomas following exposure of 291 cells to 7,12-dimethylbenz[α]anthracene in vitro as described previously (22, 25, 38). Tumor cells were grown in minimum essential medium as described above except without conditioning or epidermal growth factor and with native fetal calf serum and 1.4 mM Ca^{2+} (designated high- Ca^{2+} [HC] conditions). Clone 119 was derived by transfection of carcinoma 291.03RAT with a plasmid containing a genomic clone of mutant p53 (pmMTval135-23), obtained from Moshe Oren. It expresses predominantly wt p53 conformation (PAb246 reactive [PAb246⁺]) at 37°C (21a).

Antibodies. Mouse monoclonal antibodies to p53 were PAb421 and PAb246 (Oncogene Science, Uniondale, N.Y.). Isotype immunoglobulin G2a (IgG2a) (PAb421) and IgG1 (PAb246; Becton Dickinson, Mountain View, Calif.) were used as serum controls. Rabbit polyclonal antibody CM5 was a gift from David Lane. Antipeptide antibody to the terminal 17 amino acids unique to p53as (Fig. 1) was generated as follows. The 17-amino-acid peptide to p53as was synthesized by the RPCI Biopolymer Facility and determined to be 90 to 95% pure by high-pressure liquid chromatography and mass spectroscopy and accurate by amino acid sequencing. Following collection of preimmune serum, New Zealand White female rabbits were immunized by intradermal injection of 500 μg of peptide plus Freund's complete adjuvant at multiple sites, concurrent with intramuscular injection of pertussis vaccine

(RPCI Springville Laboratories). After 3 weeks, an additional 250 μg of peptide was administered with Freund's incomplete adjuvant at weekly intervals for 3 weeks. The p53as anti-peptide serum was affinity purified by coupling 4.4 mg of p53as peptide to an AminoLink column (Pierce, Rockford, Ill.) as specified by the manufacturer. Ammonium sulfate (40%)-precipitated preimmune serum was used as a control. Competition assays were performed by incubation of antibodies (1:1 ratio by weight) with p53as peptide (sequence shown in Fig. 1) or an unrelated peptide (GRNDCIIDKIRRNCD) for 2 h at room temperature prior to the immunoreaction with cells or peptide in enzyme-linked immunosorbent assays (ELISAs). Reactivity of anti-p53as with p53as but not p53 protein, and of PAb421 with p53 but not p53as protein, also was demonstrated by *in vitro* translation of each protein from its respective sense RNA in reticulocyte lysates, followed by immunoprecipitation with anti-p53as or PAb421 (27a).

ELISA. Nunc-Immuno MaxiSorb 96-well plates (Nunc, Roskilde, Denmark) were coated (50 ng per well) with p53as in 15 mM sodium carbonate buffer (pH 9.6). After blocking with 2% bovine serum albumin (BSA; Kirkegaard & Perry Laboratories, Gaithersburg, Md.) in phosphate-buffered saline (PBS) at 37°C for 1 h, anti-p53 monoclonal antibody, anti-p53as antibody (affinity purified to peptide), or preimmune serum control was diluted 1/50 to 1/640,000 and added to the wells in a 100- μl volume. Secondary antibody was peroxidase-conjugated goat anti-rabbit immunoglobulin (DAKO, Carpinteria, Calif.) at 1/1,000. TMB (3,3',5,5'-tetramethylbenzidine) peroxidase substrate system solution (Kirkegaard & Perry Laboratories) was added, and color development was terminated after 4 min, using 4 M H_2SO_4 . A_{450} was detected by using a plate reader (BioTek, Winooski, Vt.).

Immunofluorescence. Cells were permeabilized with 100% cold ethanol, rehydrated in PAB (PBS, 0.1% sodium azide, 0.5% BSA)–0.05% Tween 20 for 10 min, blocked with 5% normal goat serum (Vector Laboratories, Burlingame, Calif.), and then exposed to monoclonal anti-p53 antibody PAb421 or PAb246 or control isotype serum IgG2a or IgG1 (10 $\mu\text{g}/\text{ml}$ each) overnight at 4°C. Secondary antibody for monoclonal antibodies was a 1/300 dilution of fluorescein isothiocyanate (FITC)-conjugated goat anti-mouse immunoglobulin (Fisher-Biotech, Pittsburgh, Pa.). Affinity-purified rabbit polyclonal anti-p53as or ammonium sulfate-fractionated preimmune serum as a control was used at 7 $\mu\text{g}/\text{ml}$, followed by 1/300 Texas red-conjugated goat anti-rabbit immunoglobulin (Oncogene Science). FluorSave aqueous mountant (Calbiochem, La Jolla, Calif.) was used to attach coverslips to slides. The fluorescence was viewed by using a Nikon Labophot microscope equipped with epi-illuminescence. Photomicrographs were taken with a Nikon UFX-IIA automatic camera system.

Immunoprecipitation. Preconfluent cultured cells (approximately 5×10^6 to 10×10^6 cells per 100-mm-diameter petri dish) were incubated with 200 μCi of L-[^{35}S]methionine (1,120 Ci/mmol) for 4 h at 37°C in methionine-free minimum essential medium containing 2% (vol/vol) dialyzed calf serum. Labeled cells were lysed in buffer containing 1% (vol/vol) Nonidet P-40, 150 mM NaCl, 50 mM Tris (pH 8), and 1 mM phenylmethylsulfonyl fluoride for 30 min at 4°C and centrifuged at $10,000 \times g$ for 10 min. The supernatant was pre-cleared with formalin-fixed *Staphylococcus aureus* cells (Immunoprecipitin; Bethesda Research Laboratories, Gaithersburg, Md.) or with protein A-Sepharose (Pharmacia, Piscataway, N.J.). Lysate volumes corresponding to equal amounts of radioactivity (2×10^7 cpm) were incubated in NET-gel buffer (150 mM NaCl, 5 mM EDTA, 50 mM Tris [pH 7.4], 0.05% Nonidet P-40, 0.02% NaN_3 , 0.25% gelatin) for 16 h at 4°C with

antibodies to murine p53 or isotype or serum controls. Immune complexes were precipitated with Immunoprecipitin or 5 mg of protein A-Sepharose CL-4B (Pharmacia) for 2 h at 4°C and centrifuged at $10,000 \times g$ for 10 min. The pellets were washed with NET-gel buffer and eluted in loading buffer (2% [wt/vol] sodium dodecyl sulfate [SDS], 10% [vol/vol] glycerol, 125 mM Tris-Cl [pH 6.8], 0.001% [wt/vol] bromophenol blue) by heating at 85°C for 5 to 15 min and centrifugation at $10,000 \times g$ for 10 min. Supernatants were loaded on a denaturing polyacrylamide gel composed of 4% stacking gel (125 mM Tris-Cl [pH 6.8], 0.1% [wt/vol] SDS) and 10% separating gel (375 mM Tris-Cl [pH 8.8], 0.1% [wt/vol] SDS) and subjected to electrophoresis at 35 mA in running buffer (125 mM Tris-Cl [pH 8.3], 192 mM glycine, 0.1% [wt/vol] SDS). Gels were fixed in 7.5% (vol/vol) acetic acid–25% (vol/vol) methanol, soaked in enhancer solution (NEN, Boston, Mass.), and dried prior to exposure to XAR film (Kodak, Rochester, N.Y.) at -80°C with intensifying screens.

Treatment with actinomycin D. Cells on coverslips were treated with 0.25 or 0.5 nM actinomycin D (Sigma, St. Louis, Mo.) or 0.2% acetone for 48 h, beginning 24 h after plating, and stained by indirect immunofluorescence as described above. For flow cytometry or isolation of cellular RNA, approximately 2×10^4 to 3×10^4 cells per cm^2 were seeded in 150-mm-diameter plates, grown to 70% confluence, and treated with 0.5 nM actinomycin D for 48 h before harvest.

Northern (RNA) blot analysis. RNA was isolated from cells approximately 70 to 100% confluent by guanidinium-cesium chloride extraction and dissolved in diethylpyrocarbonate-treated water for Northern blot analysis as described previously (18). A 500-bp *Pst*I fragment of p53-422 was used for p53 detection (34), and a 840-bp *Eco*RI-*Sall* fragment of pA6 was used for 7S RNA detection as a control for RNA loading (2). Probes were labeled with [α - ^{32}P]dCTP by the random primer method, using a multiprime labeling kit (Amersham, Arlington Heights, Ill.). ^{32}P -labeled probe was used at a final concentration of 1×10^6 to 2×10^6 cpm/ml. Differences in p53 RNA abundance were quantitated by densitometry of exposed films (Fastscan computing densitometer; Molecular Dynamics, Sunnyvale, Calif.) after adjustment for 7S RNA.

Flow cytometry. Cells permeabilized in suspension with 100% cold ethanol were exposed to anti-p53 antibodies as described above for indirect immunofluorescence except that the secondary reagent for anti-p53as was phycoerythrin (PE)-conjugated goat anti-rabbit IgM and IgG (Fisher-Biotech). Hoechst 33342 (1 $\mu\text{g}/\text{ml}$; bisbenzimidazole H; Calbiochem) was added 1 h prior to flow analysis for detection of DNA content. Analysis was performed on a FACSTAR+ dual 5W argon laser system (Becton Dickinson Immunocytometry Systems, San Jose, Calif.) with the primary laser lasing at 488 nm at 200 mW and the secondary laser lasing at 350 nm at 50 mW. PE and Hoechst emissions were passed through discretion filters with band widths of 575 ± 13 and 424 ± 22 nm, respectively. Flow cytometry data were acquired by using Becton Dickinson standard acquisition software to exclude cell aggregates and debris and to collect single-cell events only. Data were analyzed with Lysis II software (Becton Dickinson Immunocytometry Systems).

RESULTS

To determine whether the p53as protein was made in cells, a polyclonal antibody to the 17-amino-acid sequence unique to p53as was generated in rabbits. Rabbit serum collected at intervals after immunization was tested for reactivity to p53as peptide coated on ELISA plate wells (Fig. 2). High-titer serum

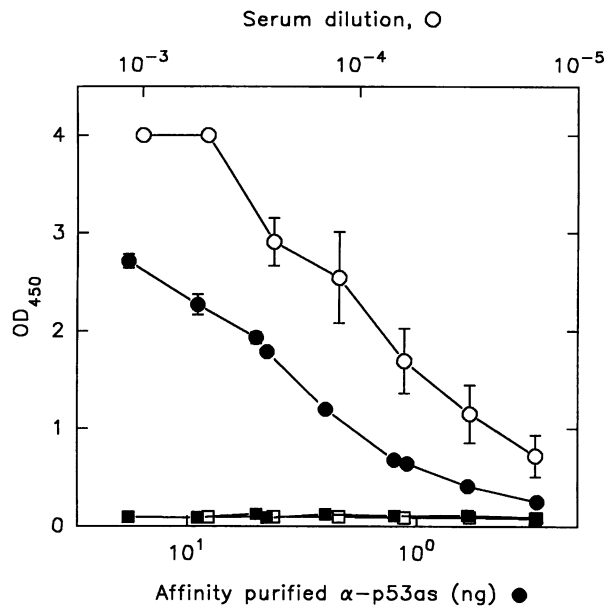


FIG. 2. Reactivities with p53as peptide of anti-p53as serum and affinity-purified antibody detected by ELISA. New Zealand White female rabbits were immunized with a peptide equivalent to the C-terminal 17 amino acids of p53as. ELISA plates were coated with 50 ng of peptide per well and reacted in duplicate with preimmune serum or day 63 immune serum at 1/500 through 1/640,000 (1/2 dilutions) and peroxidase-conjugated, affinity-isolated goat anti-rabbit immunoglobulin. Whole immune serum (open circles; four experiments) or affinity-purified (to the peptide) anti-p53as antibody (α -p53as; closed circles; two experiments) was used as the primary antibody, and whole preimmune serum (open squares) or ammonium sulfate-precipitated IgG fraction (closed squares) was used as a control. OD₄₅₀, optical density at 450 nm.

(Fig. 2) was affinity purified against the 17-amino-acid peptide. The reactivity (per 50 ng of antigen) of 10 ng of affinity-purified antibody was approximately equivalent to a 1/40,000 dilution of whole anti-p53as antiserum. Anti-p53as reactivity in the ELISA and indirect immunofluorescence assays was blocked competitively by preincubation of antibody with the p53as peptide.

Immunoprecipitation. To determine its reactivity with cellular proteins, affinity-purified antiserum to p53as was reacted with mouse epidermal cell lysates (Fig. 3). A 53-kDa protein was immunoprecipitated by anti-p53as. This protein migrated slightly faster on 10% polyacrylamide gels than p53 protein immunoprecipitated by PAb421 (which binds to a carboxyl-terminal epitope absent in p53as). Rabbit polyclonal anti-p53 antibody CM5 recognized a broader band spanning the region containing more discrete PAb421⁺ and anti-p53as⁺ reactive forms.

Indirect immunofluorescence. The location and incidence of expression of p53as in cell populations grown on coverslips were determined by indirect immunofluorescence. As shown in Fig. 4, nuclear staining was observed with affinity-purified anti-p53as antibody. This activity was completely blocked by competitive binding with p53as peptide (Fig. 4C). Anti-p53as antibody reactivity in 291 nontransformed cells and carcinoma cells was always nuclear under the conditions of these assays (data for clone 119 are shown) and in this respect was like PAb246 antibody reactivity. This was true even in clones of 291.03RAT transfected with the pmMTval-135 temperature-

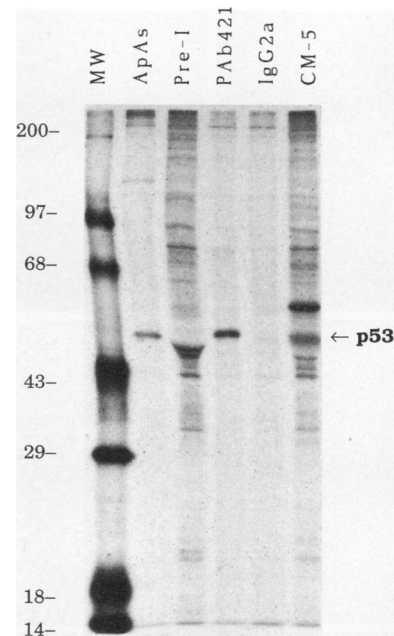


FIG. 3. Anti-p53as immunoprecipitation of a 53-kDa protein. For immunoprecipitation of p53as from squamous cell carcinoma line 291.03RAT, [³⁵S]methionine-labeled cells were lysed, and 2×10^7 cpm of lysate was reacted with the antibodies or antisera indicated. Lanes: MW, molecular mass standards (sizes are indicated in kilodaltons); ApAs, affinity-purified anti-p53as; Pre-I, preimmune rabbit serum; PAb421, anti-p53 antibody to an epitope absent in p53as; IgG2a, mouse IgG isotype control for PAb421; CM-5, rabbit polyclonal anti-p53 antibody CM5 reactive with both p53 and p53as proteins. After separation from the antibody complex by heating at 85°C for 5 min, proteins were resolved by electrophoresis as described in Materials and Methods. Proteins of 53 kDa were detectable by PAb421, affinity-purified anti-p53as, and rabbit polyclonal anti-p53 serum CM5.

sensitive mutant of p53, in which PAb421 reactivity was cytoplasmic as well as nuclear. These results suggest that like the major p53 form, wt p53as protein exerts its effects primarily in the nucleus.

p53 expression in nontransformed cells and tumor cells. We reported previously that squamous cell carcinoma 291.03RAT expresses 3-fold more p53 mRNA and up to 10-fold less p53 protein (PAb421 and PAb246 antibody reactivity) than the progenitor 291 cells (16). Comparison of the expression of p53as protein in these cell lines was done by immunoprecipitation. As shown in Fig. 5, reactivity with anti-p53as antibody was detected in nontransformed 291 cells and carcinoma cells. The p53as-precipitable protein in these cell lines migrates slightly faster than the PAb421- and PAb246-precipitable proteins, as expected from the truncation of p53as by nine carboxy-terminal amino acids (expected to result in an approximately 1-kDa difference in molecular mass). As expected from previous studies (16), immunoreactivity to all three anti-p53 antibodies was lower in 291.03RAT carcinoma cells than in normal cells. The ratio of immunoprecipitable protein in populations of proliferating cells versus differentiating 291 cells was higher for anti-p53as (5/1) and for PAb421 (2/1) than for PAb246 (1/1). Elevated PAb421 reactivity in proliferating populations also was noted by Milner (29) in studies of mouse lymphocytes. These results suggested that p53as protein might be differentially expressed relative to PAb421 and PAb246

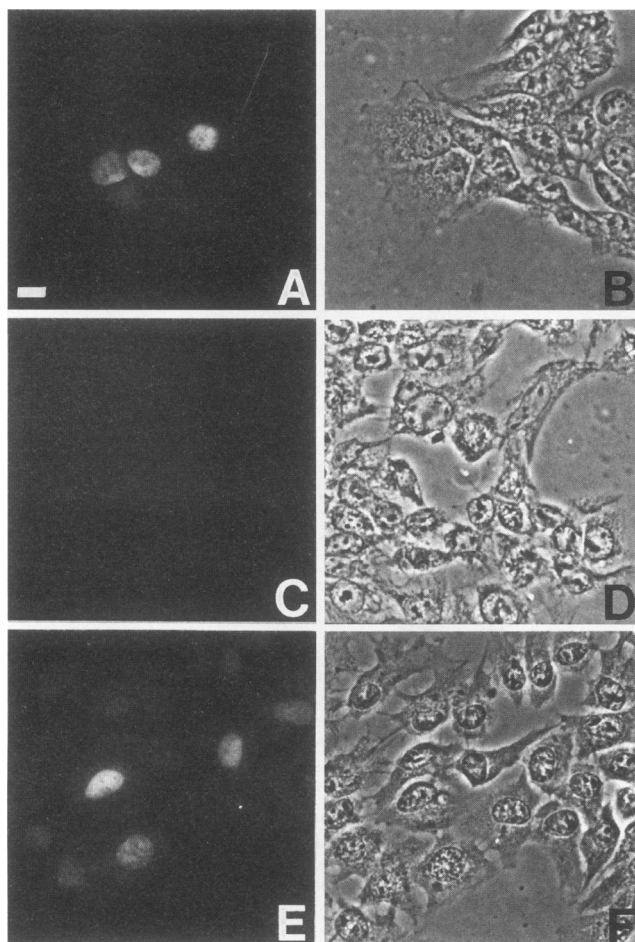


FIG. 4. Nuclear localization of p53as antigen activity. Cells were plated at 1.5×10^4 cells per cm^2 on glass coverslips and grown until about 70% confluent. Nuclear reactivity was detected by using affinity-purified anti-p53as antibody in indirect immunofluorescence assays of 100% ethanol-fixed cells (A). This reactivity was completely blocked by competition with a 1:1 ratio (by weight) of the 17-amino-acid peptide corresponding to the C terminus of the p53as protein (C). No competition was evident with up to a 10:1 ratio of an unrelated 16-amino-acid peptide (E). Phase-contrast optics corresponding to the immunofluorescence field are shown in panels B, D, and F. Findings were similar for all epidermal cell lines (transfectant clone 119 of 291.03RAT is shown). Fluorescence in IgG2a, IgG1, or ammonium-sulfate fractionated preimmune serum controls was negligible (data not shown). Bar equals 10 μm .

protein, dependent on cellular proliferative or differentiative states.

Response to actinomycin D. p53 protein has been postulated to participate in a cell cycle checkpoint regulating entry into S phase after exposure of cells to DNA-damaging agents such as actinomycin D (20, 21, 27). Cells expressing wt p53 (PAb421 reactivity) arrest in the G_1 stage of the cell cycle following DNA damage, and p53 immunoreactivity is coordinately increased. Prior to studies of the cell cycle distribution of p53as⁺ epidermal cells, experiments were performed to determine whether p53as protein also may respond to DNA damage, to determine whether it was possible thereby to maximize the percentage of p53as⁺ cells in the cell population, and to compare the responses of nontransformed and malignant epidermal cells. Moderately differentiated squamous cell car-

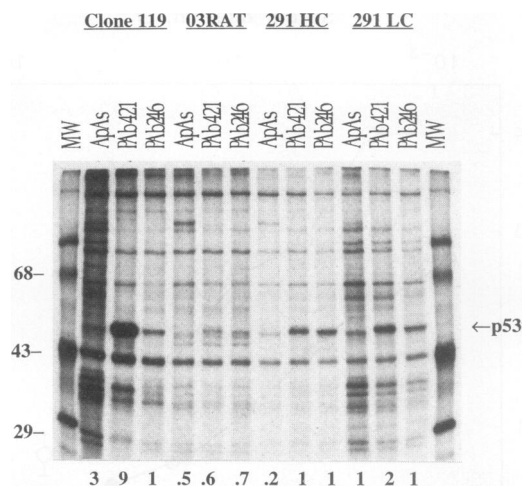


FIG. 5. Comparative immunoprecipitation of p53 from proliferating (LC) or differentiating (HC) nontransformed parental 291 cells and from 291.03RAT (03RAT) carcinoma cells or its derivative clone 119 transfected with a mutant p53 (valine 135). Cell lysates were incubated with 2 μg of PAb421, 4 μg of PAb246, or 1.4 μg of anti-p53as (ApAs) in NET-gel. Immunocomplexes were incubated with 5 mg of protein A for 2 h at 4°C and centrifuged, and immunoprecipitated protein was eluted from pellets with heating at 85°C for 15 min. After centrifugation, proteins in the supernatants were separated by electrophoresis on a 10% polyacrylamide denaturing gel with molecular mass standards (lane MW; sizes are indicated in kilodaltons). To assist in comparisons of a particular antibody reactivity among the cell lines, the densities of the p53 signal in each lane are provided (numbers at the bottom) relative to anti-p53as reactivity of 291 LC as 1.

cinoma line 291.05RAT was used for these studies because it expressed higher levels of immunoprecipitable p53 protein than 291.03RAT does but, like 291.03RAT, is derived from epidermal clone 291 and has the wt p53 gene (16). Treatment with actinomycin D induced p53 and p53as protein expression in two separate experiments, as judged from the percentage of cells positive for reactivity with p53 antibodies by indirect immunofluorescence (Table 1). The increase in positive cells was less for p53as than for PAb421 and PAb246 reactivities and required a higher concentration of actinomycin D, but this may reflect the lower abundance of p53as protein. As in untreated 291 epidermal cells and in the 291.03RAT tumor cells expressing wt p53, the p53as antibody reactivity in actinomycin D-treated cells was nuclear. Most of the p53as-positive nuclei were also positive for PAb421 or PAb246, whereas most PAb421⁺ or PAb246⁺ cells were negative for p53as antibody reactivity. The abundance of p53 RNA in actinomycin D-treated 291.05RAT cells was increased over threefold, as judged by Northern blot analysis (data not shown), suggesting that the response of epidermal cells to actinomycin D involves increases in RNA abundance. The increase in abundance of p53 antibody reactivity following actinomycin D treatment was similar to the response of ML-1 and normal myeloid progenitor cells to γ rays reported by Kastan et al. (20). The current findings are consistent with a functional role for p53as protein along with p53 protein in cellular response to actinomycin D.

Flow cytometry. The elevation of wt p53 coordinated with G_1 arrest of cells in response to various DNA-damaging agents suggested a role as a G_1/S cell cycle checkpoint permitting time for repair of DNA damage or induction of programmed cell

TABLE 1. Response of 291.05RAT epidermal tumor cells to actinomycin D detectable by indirect immunofluorescence^a

Expt	Treatment	p53-positive cells (%)		
		PAb421	PAb246	Anti-p53as
1	Acetone, 0.2%	5-7	2-3	1-6
	Actinomycin D, 0.5 nM	72-75	57-60	40-60
2	Acetone, 0.2%	6-8	3-5	1-5
	Actinomycin D, 0.25 nM	25-50	40	3-5
	Actinomycin D, 0.5 nM	70-80	70-80	15-20

^a Cells were plated on coverslips, treated as indicated for 48 h, and then stained with p53 antibodies. Estimates of positive cells as a percentage of total cells were made on the basis of viewing all cells per slip (10 control and 8 to 10 treated slips per experiment for anti-p53as; 4 control and 2 to 4 treated slips per experiment for PAb421; 2 control and 2 treated slips per experiment for PAb246, preimmune, and IgG controls). The ranges of percent positive cells for two independent experiments are shown.

death in severely damaged cells (27). Flow cytometry was performed to determine whether p53as antigen activity was differentially expressed during the cell cycle. Cells which had been exposed to actinomycin D or solvent were stained with antibodies to p53as and PAb421 or PAb246, taking advantage of the different species of origin of the polyclonal and monoclonal antibodies to permit immunodetection of p53as and p53 antigens in the same cell. PE (red) conjugated to anti-rabbit immunoglobulin was used to recognize p53as, and FITC (green) conjugated to anti-mouse immunoglobulin was used to recognize PAb421 and PAb246. Coordinates were set on the basis of the fluorescence intensity in primary antibody controls (Fig. 6A and 7A) to detect events (single cells) positive for anti-p53as reactivity alone (region 1 [R1]), positive for anti-p53as and PAb421 or PAb246 (R2), negative for anti-p53as and positive for PAb421 or PAb246 (R3), and negative for both anti-p53as and PAb421 or PAb246 (R4). Cells positive for anti-p53as alone (R1), when present, showed a distribution of DNA content similar to that of cells positive for p53as and PAb421 or PAb246. Competition with p53as peptide, but not an unrelated peptide, effectively blocked events detectable in R1 and R2 (shown for 291.05RAT in Fig. 6B, C, E, and F and for 291 cells in Fig. 7B, C, E, and F) without appreciably affecting the R3 events, verifying the specificity of the anti-p53as antibody for p53as protein and its lack of reactivity with the major p53 protein. Thousands of events from each region were collected for analysis of cell cycle distribution according to Hoechst area, represented in the histograms (Fig. 6G to I and 7G to I for R2, R3, and R4, respectively). The cell cycle distributions of actinomycin D-treated 291.05RAT cells (shown) and controls were essentially the same. The cells negative for both antibody reactivities (Fig. 6I and 7I) and the PAb421⁺ p53as⁻ cells (Fig. 6H and 7H) were distributed primarily in the G₀/G₁ phase of the cell cycle, while p53as⁺ cells (Fig. 6G and 7G) were preferentially in the G₂/M phase of the cycle. Particularly striking is the distribution of p53as⁺ cells in a tail, indicating DNA content in excess of that in G₂/M cells. Since single cells only were collected for analysis, it is likely that such cells had undergone DNA synthesis or even nuclear division but failed to undergo cytokinesis. Inspection of p53as⁺ cells grown on coverslips revealed that most (approximately 85%) contained two or more nuclei (data not shown), supporting the conclusion that these carcinoma cells continued to synthesize DNA and to undergo nuclear division

but failed to undergo cell division. Nontransformed 291 cells, cultured under conditions favoring proliferation (LC), were treated similarly for comparison with carcinoma cells (Fig. 7). The p53as⁺ 291 cells (whether singly or also positive for PAb421) were preferentially in the G₂/M stage, while PAb421⁺ cells were preferentially in G₀/G₁. Unlike the carcinoma cells, the p53as⁺ 291 cells observed on coverslips were mononucleated (data not shown). Nontransformed and carcinoma cells positive for PAb246 reactivity showed cell cycle distributions essentially the same as that of cells positive for PAb421.

The percentage distributions by cell cycle stage of nontransformed 291 and 291.05RAT carcinoma cells treated with actinomycin D or solvent controls are presented in Table 2. The preferential association of p53as antigen activity with G₂/M and >G₂/M and the association of p53 protein (reactive with PAb421 and PAb246) with G₀/G₁ was consistent in all experiments. In nontransformed 291 cells, actinomycin D increased the percentage of cells expressing immunodetectable p53as and p53 (PAb421 and PAb246) by approximately fourfold. Also, in response to actinomycin D, the distribution of p53as⁺ cells changed in favor of G₀/G₁, suggesting that both p53as and the p53 protein reactive with PAb421 and PAb246 contribute to G₁ arrest in normal cells exposed to DNA damage. The 291.05RAT tumor cells also demonstrated increases in the percentages of cells positive for anti-p53as (up to 17-fold compared with controls), PAb421, and PAb246 following actinomycin D treatment. In contrast to the 291 cells, however, the 291.05RAT cells showed little difference in the percentage of cells in G₁ in response to actinomycin D treatment, suggesting that the p53 protein in these cells was less capable of causing G₁ arrest, even though the percentages of PAb421⁺ and PAb246⁺ cells were elevated.

DISCUSSION

p53as, a physiological variant of the tumor suppressor protein p53, has been detected in mouse epidermal cells containing the wt p53 gene. The fact that endogenous wt p53as protein has not been detected in cells before may be due to its low abundance and lack of reactivity with anti-p53 monoclonal antibody PAb421. We showed previously that the wt p53as mRNA is present in normal mouse tissues and in cultured mouse fibroblasts at 25 to 33% of the level of the major p53 RNA form (17). The current studies demonstrated that the p53as protein exists in cells, was nuclear in location in normal epidermal and carcinoma cells, was differentially expressed in proliferating compared with differentiating cultures of nontransformed cells, was preferentially expressed in the G₂ phase of the cell cycle, and was inducible along with PAb421- and PAb246-reactive p53 by actinomycin D.

The distribution of p53as⁺ cells in G₂/M and >G₂/M appears likely to reflect a growth arrest or maturation pathway, yet immunodetectable p53as was expressed preferentially in proliferating cells. This finding could suggest that p53as is involved in maintaining the balance between growth and maturation within epidermal cell populations. Even under conditions favoring proliferation (LC conditions; see Materials and Methods), basal (proliferation-associated) cell markers are lost with time after plating, and differentiating cells increase as a percentage of the total population (24). We have reported previously that mouse keratinocytes exhibit a bimodal DNA content, containing stable populations of 2N and 4N DNA content 3 to 19 days after establishment in primary culture (23). While the 291 cells are subtetraploid (26), they appear to retain the capacity to generate a subpopulation of

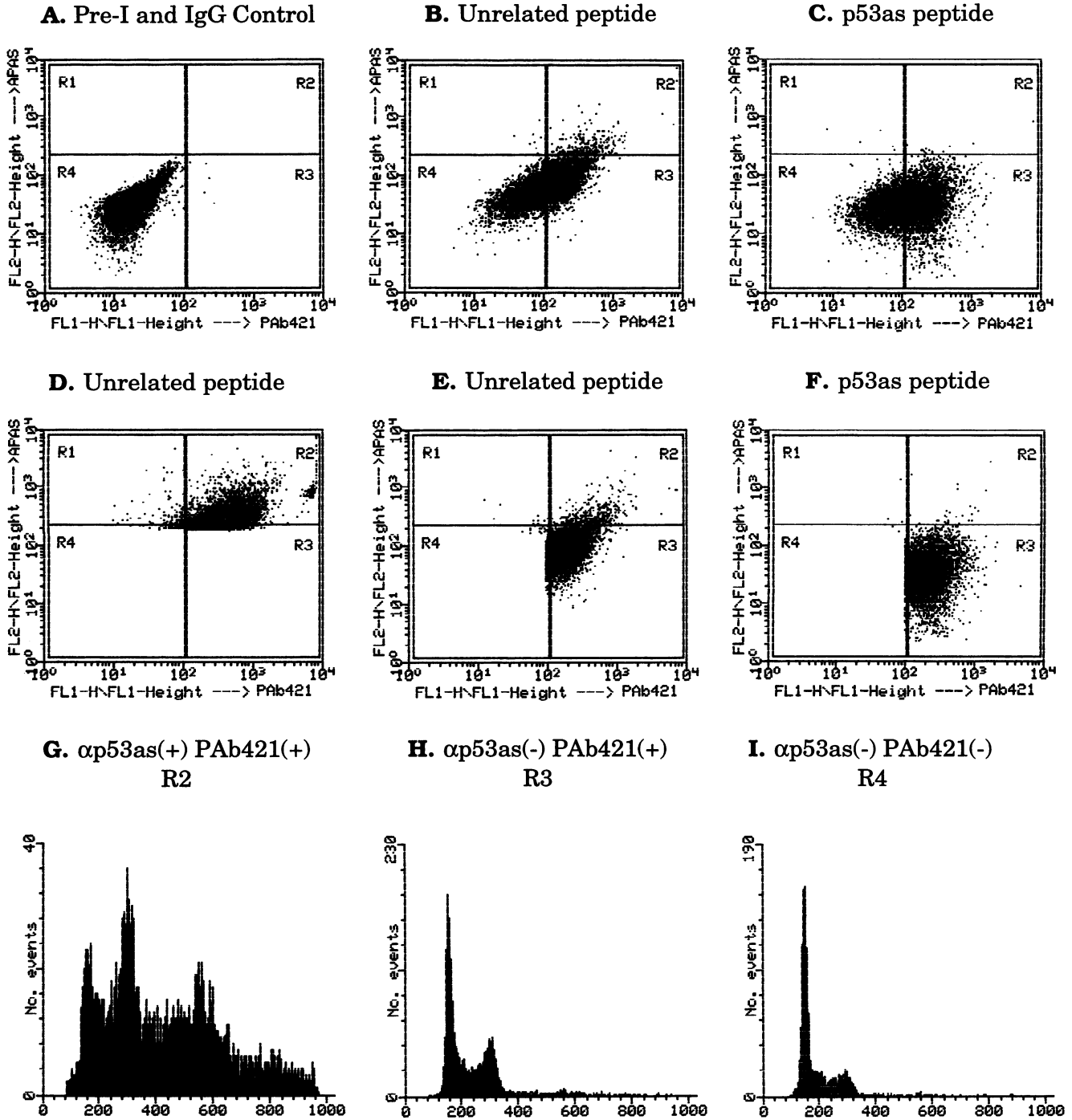


FIG. 6. Expression of p53 (PAb421) and p53as antigen activities in 291.05RAT carcinoma cells. Cells were treated with 0.5 nM actinomycin D for 2 days and harvested by trypsinization. Cells were permeabilized and stained in suspension with anti-p53as (α p53as) and PAb421 antibodies (in the same tube) in all cases shown except for the primary antibody control (A). In the dot plots (A to F), the FL1 fluorescence intensity on the x axis was FITC (green), used to visualize PAb421 reactivity, and the FL2 fluorescence intensity on the y axis was PE (red), used to visualize anti-p53as reactivity. Prior to incubation with cells, the anti-p53as antibody was exposed either to p53as peptide (C and F), which competitively removed the specific anti-p53as reactivity, or to an unrelated peptide (B, D, and E), which controlled for nonspecific binding to peptide, leaving only specific reactivity to p53as protein. Events collected by flow cytometry were single cells only as described in Materials and Methods. Coordinates were set on total cell data based on IgG2a and preimmune (Pre-I) controls to delineate four regions: negative for both antibodies (R4), positive for anti-p53as only (R1), positive for PAb421 and anti-p53as (R2), and positive for PAb421 only (R3). The cell cycle distributions of events from regions R2, R3, and R4 are shown in the histograms in panels G to I. After collection of a file of 10,000 total events per tube (as shown in panels A to C), additional gates were set which excluded negative cells (R4) (as shown in dot blot E, used to generate the histogram for PAb421⁺ cells shown in panel H) or excluded negative cells (R4) and cells positive for PAb421 (R3) (as shown in dot blot D, used to generate the histogram for p53as⁺ cells shown in panel G). The numbers of cells in each region expressed as a percentage of the total cells were as follows:

cells with increased DNA content. Davies et al. (8) have discussed the changes in ploidy from 2N to 4N and 8N which occur by DNA doubling without cytokinesis and accompany the maturation of normal liver cells. The presence of cells with $\geq G_2/M$ DNA content in epidermal cell populations could similarly reflect a maturation pathway.

The increase in percentage of p53as⁺ 291 nontransformed cells in response to actinomycin D suggests that p53as protein cooperates with p53 detectable by PAb421 and PAb246 in the G₁ arrest induced by DNA damage. Although the percentage of p53⁺ cells generally was increased following actinomycin D treatment, 291.05RAT carcinoma cells were deficient in G₁ arrest and p53as⁺ cells did not undergo a shift in distribution from the G₂ phase to the G₁ phase of the cell cycle, suggesting that p53 protein in the carcinoma is defective in cell cycle arrest. However, the preferential association of p53as protein immunoreactivity with G₂/M occurs in control and in actinomycin D-treated cells, suggesting that it reflects a physiological activity of p53as protein associated with the G₂ stage rather than a consequence of treatment. It is intriguing that actinomycin D and γ -ray treatments induce G₁ and G₂ arrest, but only G₁ arrest is associated with a rise in PAb421 activity (20). One could speculate that p53as protein has a role in G₂/M arrest in response to DNA damage. The observation that most p53as⁺ carcinoma cells were multinucleated whereas most p53as⁺ nontransformed cells were mononucleated supports the idea that tumor cells may have a defect in the ability to lengthen G₂ and delay nuclear division following DNA damage.

Additional inferences about the functional properties of p53as protein can be made from the studies of others. Changes at the carboxyl terminus of p53 protein engineered by site-directed mutagenesis or deletion mapping have been shown to have dramatic effects on p53 structure and function (19). Sturzbecher et al. (43) demonstrated that loss of C-terminal basic residues permitted dimer formation of p53 protein but not tetramers, while Hainaut and Milner (15) showed that similarly, deletion of 25 C-terminal amino acids of p53 resulted in dimers but not higher-order complexes. Since p53 protein is thought to bind to DNA as a tetramer (3, 41), restriction of p53as to dimer formation may influence its interactions with DNA.

Properties of the mutated form of alternatively spliced p53 protein translated in vitro from the M-8 cDNA clone (1) have been reported. Hainaut and Milner (15) observed that following in vitro translation, the mutant alternatively spliced p53 protein encoded by M-8 formed monomers and dimers but not tetramers. Like the mutant M-8 protein, wt p53as has lost the basic amino acids of the C terminus but retains the acidic amino acids shown to permit dimer formation. These results support the idea that wt p53as may have distinct properties from the major p53 protein form. However, the M-8 p53 cDNA sequence has a nucleotide substitution at nucleotide 395 resulting in a change from cysteine 132 to phenylalanine. Elyahu et al. (9) reported that plasmids containing the M-8 p53 cDNA had transforming activity in transfected cells.

Mutations within this region without alternative splicing give rise to p53 proteins defective in tumor suppressor function and DNA binding (references 9, 11, and 45 and references therein). Thus, the M-8 protein has a mutation which affects its function apart from the C-terminal changes due to alternative splicing. p53 protein translated from cDNA clone M-8 does not react with PAb248 antibody, which like PAb246 is wt conformation specific, or, as a result of loss of the C-terminal epitope, PAb421 (48). Since wt p53as has a distinct conformation compared with the mutated M-8 protein, functional properties such as DNA binding cannot be predicted from studies of M-8 protein and must be tested directly.

In addition to alterations in the oligomerization domain predicted from the studies described above, p53as has lost the casein kinase II phosphorylation-5.8S rRNA binding site located at serine 389 (Fig. 1). Loss of the phosphorylation site at serine 389 by mutation negates p53 antiproliferative activity (4, 28, 33). Hupp et al. (19) have shown that factors acting at the C terminus are important for activation of the DNA binding capacity of wt p53, including phosphorylation at the conserved C-terminal serine, PAb421 antibody binding to its carboxy-terminal epitope, and proteolysis or engineered loss of the last 30 carboxy-terminal amino acids. In addition, regions of the p53 protein which mediate binding to other cellular proteins such as heat shock protein (6, 15) or mdm2 (32) conceivably could be directly or (by conformational changes) indirectly altered in p53as protein.

The differential expression of p53 and p53as protein immunoreactivities during the cell cycle suggests that each has a distinct function. Perhaps p53 may prove to be within the class of transcription factors which generate two functionally distinct proteins by alternative splicing (14). For example, in the case of mouse TFE3 (transcription factor E3) (which regulates immunoglobulin transcription by binding to promoter and enhancer regions), there is a longer and a shorter protein form. In the shorter form, amino acids predicted to form an amphipathic helix are absent and transcriptional activation activity is affected. The ability of such factors to heterodimerize amplifies the possibilities for regulation of expression of target genes.

It will be important to determine the activity of wt p53as in tumor suppression. While originally thought to be an oncogene because initial clones of p53 harbored mutations, cloning of wt p53 led to the recognition of its role as a tumor suppressor gene (9, 11). The capacity of mutant p53 protein to drive wt p53 into the mutant conformation uncovered its potential as a dominant negative transforming gene (29, 31). Yet mutant p53 itself has transforming activity in cells which have no wt p53, suggesting direct activities of p53 in the regulation of proliferation (49). Milner (30) has proposed that p53 has positive and negative functions in cell cycle regulation, dependent on p53 conformation. One could speculate that positive or negative functions of p53 in regulation of cell cycle progression or induction of apoptosis may reside in the relative expression of different physiological variants of p53 generated by alternative splicing. Studies to compare differential functional activity of the wt p53 and p53as in DNA binding, transcriptional activa-

control (A), R1, 0, R2, 0, R3, 0.5, and R4, 100 (numbers may not add to 100 because of rounding error and a negligible number of events outside the windows included in the analysis); unrelated peptide (B), R1, 0.1, R2, 3, R3, 47, and R4, 47; and p53as peptide (C), R1, 0.05, R2, 0.2, R3, 53, and R4, 44. The numbers of events in each gated region shown were as follows: R1, 142, and R2, 6,339 (D); R1, 10, R2, 453, and R3, 8,309 (E); and R1, 3, R2, 28, and R3, 8,816 (F). Note that the total numbers of events in panels E and F are comparable, indicating the specificity of the anti-p53as antibody for p53as antigen and lack of cross-reactivity with p53 antigen. The percentages of cells in each phase of the cell cycle and total events (*n*) for each region in the histograms shown were as follows: R2, G₀/G₁, 14, S, 8, G₂/M, 26, and >G₂/M, 52, *n* = 6339 (G); R3, G₀/G₁, 51, S, 14, G₂/M, 30, and >G₂/M, 5, *n* = 8309 (H); and R4, G₀/G₁, 70, S, 12, G₂/M, 16, and >G₂/M, 2, *n* = 4741 (I).

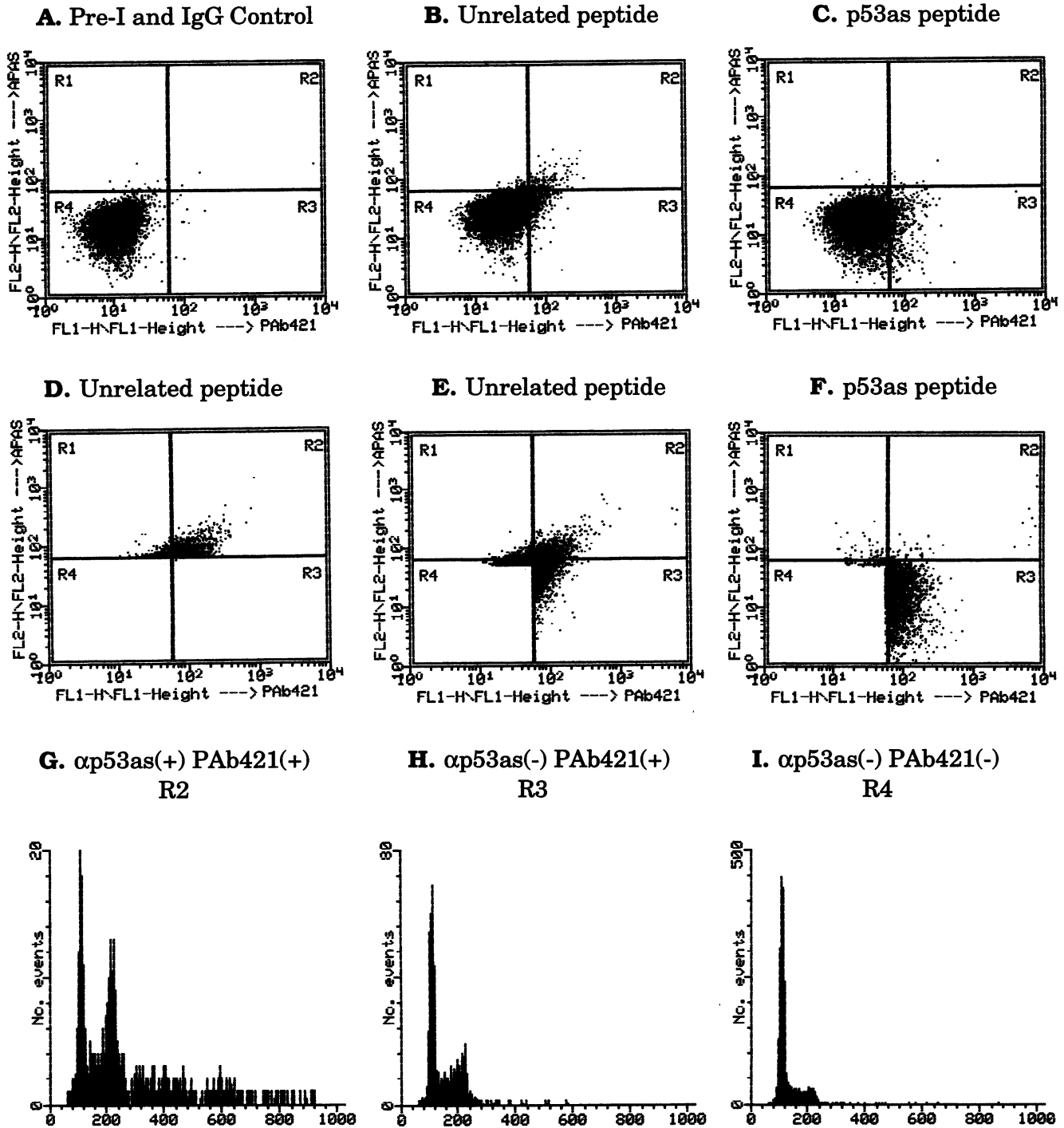


FIG. 7. Expression of p53 (PAb421) and p53as antigen activities in 291 nontransformed cells. Cells were cultured under LC conditions, which favored cell growth. Analysis was the same as for carcinoma cells presented in Fig. 6. Acetone control cells are shown. The numbers of cells in each region expressed as a percentage of the total cells were as follows: control (A), R1, 0.2, R2, 0.04, R3, 0.1, and R4, 100; unrelated peptide (B), R1, 1, R2, 2, R3, 4, and R4, 92; p53as peptide (C), R1, 0.1, R2, 0.1, R3, 5, and R4, 94. The numbers of events in each gated region shown were as follows: R1, 564, and R2, 1,074 (D); R1, 521, R2, 918, and R3, 1,974 (E); and R1, 72, R2, 62, and R4, 3,439 (F). Percentages of cells in each phase of the cell cycle and total events (n) for each region in the histograms shown were as follows: R2, G_0/G_1 , 29, S, 11, G_2/M , 35, and $>G_2/M$, 25, $n = 1,074$; R3, G_0/G_1 , 61, S, 15, G_2/M , 22, and $>G_2/M$, 2, $n = 1,974$; R4, G_0/G_1 , 78, S, 11, G_2/M , 11, and $>G_2/M$, 0.04, $n = 9,194$. Designations are as described in the legend to Fig. 6.

TABLE 2. Cell cycle distribution by flow cytometry of mouse epidermal cells according to p53 antibody reactivities^a

Cells	Treatment	Stage	Distribution			
			R4 negative cells	Anti-p53as	PAb421	PAb246
291 LC	Acetone	>G ₂ /M	0.6 ± 0.2	33 ± 6	4 ± 0.6	0.3 ± 0.2
		G ₂ /M	18 ± 1	43 ± 7	30 ± 3	34 ± 2
		S	11 ± 1	9 ± 2	14 ± 3	11 ± 1
	Actinomycin D	G ₀ /G ₁	70 ± 1	15 ± 2	52 ± 1	48 ± 1
		% of total cells	100 ± 0.2	0.5 ± 0.2	8 ± 2	3 ± 0.2
		>G ₂ /M	0.3 ± 0.2	3 ± 2	0.5 ± 0.1	0.3 ± 0.2
291.05RAT	Acetone	G ₂ /M	9 ± 2	30 ± 2	10 ± 1	11 ± 1
		S	8 ± 0.9	10 ± 1	8 ± 0.4	9 ± 0.5
		G ₀ /G ₁	83 ± 2	56 ± 4	82 ± 1	80 ± 1
	Actinomycin D	% of total cells	100 ± 0.6	2 ± 0.8	36 ± 3	12 ± 1
		>G ₂ /M	1 ± 0.4	23 ± 6	8 ± 1	6 ± 0.5
		G ₂ /M	19 ± 2	30 ± 5	32 ± 4	29 ± 1
291.05RAT	Acetone	S	22 ± 2	25 ± 5	24 ± 7	19 ± 3
		G ₀ /G ₁	58 ± 3	23 ± 3	36 ± 5	46 ± 2
		% of total cells	97 ± 4	1 ± 0.4	2 ± 0.6	10 ± 2
	Actinomycin D	>G ₂ /M	1 ± 0.4	3 ± 3	1 ± 1	0.8 ± 0.1
		G ₂ /M	15 ± 3	40 ± 5	27 ± 5	26 ± 1
		S	20 ± 2	28 ± 6	24 ± 5	25 ± 1
291.05RAT	Actinomycin D	G ₀ /G ₁	64 ± 4	28 ± 4	48 ± 1	48 ± 1
		% of total cells	93 ± 9	1 ± 0.4	10 ± 0.1	23 ± 1

^a Cells were exposed to 0.5 nM actinomycin D or solvent for 2 days, harvested, and stained as described in the legend to Fig. 6 and Materials and Methods. Values are means ± standard deviations of percentages of cells positive for each antibody, based on 2×10^6 stained cells each in 12 separate tubes (R4 negative cells or total cells), 6 tubes (anti-p53as), or 2 tubes, with two separate datum files collected per tube (PAb421 and PAb246). Regions for p53as⁺ events (R1 and R2) were set conservatively in order to analyze the cell cycle of the more brightly positive cells; thus, the percentages of p53as⁺ cells in this experiment were underestimated. The results for cell cycle distribution are representative of four separate experiments for 291.05RAT and three for 291, including both actinomycin D and control groups.

tion, cellular transformation, cell cycle arrest, and apoptosis will be necessary to test these possibilities.

ACKNOWLEDGMENTS

This work was supported by Public Health Service grants CA31101, CA13038, and CA16056 from the National Cancer Institute. Hua Huang is supported by The Stanford Henderson and Bertha Scott Endowed Fellowship of RPCI.

We are grateful to Samuel Benchimol, University of Toronto, Toronto, Canada, for the PAb421 and PAb246 (obtained as the supernatant of hybridoma tissue culture) initially used in our studies; to David Lane, University of Dundee, Dundee, Scotland, for CM5 antiserum; to Moshe Oren, Weizmann Institute of Science, for the plasmid pmMTval135-23 used to derive transfectant clone 119; and to Carleton Stewart and David Sheedy for data collection and discussion of flow cytometry analysis procedures. We thank Joseph Brachman for expert immunization and collection of the anti-p53as antiserum and Karen Shrader for typing assistance.

REFERENCES

- Arai, N., D. Nomura, K. Yokota, D. Wolf, E. Brill, O. Shohat, and V. Rotter. 1986. Immunologically distinct p53 molecules generated by alternative splicing. *Mol. Cell. Biol.* **6**:3232-3239.
- Balmain, A., R. Krumlauf, J. K. Vass, and G. D. Birnie. 1982. Cloning and characterization of the abundant cytoplasmic 7S RNA from mouse cells. *Nucleic Acids Res.* **10**:4259-4277.
- Bargonetti, J., I. Reynisdottir, P. N. Friedman, and C. Prives. 1992. Site-specific binding of wild-type p53 to cellular DNA is inhibited by SV40 T antigen and mutant p53. *Genes Dev.* **6**:1886-1898.
- Bischoff, J. R., D. Casso, and D. Beach. 1992. Human p53 inhibits growth in *Schizosaccharomyces pombe*. *Mol. Cell. Biol.* **12**:1405-1411.
- Burns, P. A., C. J. Kemp, J. V. Gannon, D. P. Lane, R. Bremner, and A. Balmain. 1991. Loss of heterozygosity and mutational alterations of the p53 gene in skin tumours of interspecific hybrid mice. *Oncogene* **6**:2363-2369.
- Clarke, C. F., K. Cheng, A. B. Frey, R. Stein, P. W. Hinds, and A. Levine. 1988. Purification of complexes of nuclear oncogene p53 with rat and *Escherichia coli* heat shock proteins: in vitro dissociation of *hsc70* and *dnaK* from murine p53 by ATP. *Mol. Cell. Biol.* **8**:1206-1215.
- Crook, T., C. Fisher, and K. H. Vousden. 1991. Modulation of immortalizing properties of human papillomavirus type 16 E7 by p53 expression. *J. Virol.* **6**:505-510.
- Davies, R., R. E. Edwards, J. A. Green, R. F. Legg, R. T. Snowden, and M. M. Manson. 1993. Antioxidants can delay liver cell maturation which in turn affects γ -glutamyltranspeptidase expression. *Carcinogen* **14**:47-52.
- Eliyahu, D., N. Goldfinger, O. Pinhasi-Kimhi, G. Shaulsky, Y. Skurnik, N. Arai, V. Rotter, and M. Oren. 1988. Meth A fibrosarcoma cells express two transforming mutant p53 species. *Oncogene* **3**:313-321.
- Farmer, G., J. Bargonetti, H. Zhu, P. Friedman, R. Prywes, and C. Prives. 1992. Wild-type p53 activates transcription *in vitro*. *Nature (London)* **358**:83-86.
- Finlay, C. A., P. W. Hinds, and A. J. Levine. 1989. The p53 proto-oncogene can act as a suppressor of transformation. *Cell* **57**:1083-1093.
- Fontoura, B. M. A., E. A. Sorokina, E. David, and R. B. Carroll. 1992. p53 is covalently linked to 5.8S rRNA. *Mol. Cell. Biol.* **12**:5145-5151.
- Foord, O. S., P. Bhattacharya, Z. Reich, and V. Rotter. 1991. A DNA binding domain contained in the C-terminus of wild type p53 protein. *Nucleic Acids Res.* **19**:5191-5198.
- Foulkes, N. S., and P. Sassone-Corsi. 1992. More is better: activators and repressors from the same gene. *Cell* **68**:411-414.
- Hainaut, P., and J. Milner. 1992. Interaction of heat-shock protein 70 with p53 translated *in vitro* evidence for interaction with dimeric p53 and for a role in the regulation of p53 conformation. *EMBO J.* **11**:3513-3520.
- Han, K.-A., and M. F. Kulesz-Martin. 1992. Altered expression of wild-type p53 tumor suppressor gene during murine epithelial cell transformation. *Cancer Res.* **52**:749-753.
- Han, K.-A., and M. F. Kulesz-Martin. 1992. Alternatively spliced p53 RNA in transformed and normal cells of different tissue types. *Nucleic Acids Res.* **20**:1979-1981.
- Han, K.-A., P. Rothberg, and M. Kulesz-Martin. 1990. Altered levels of endogenous retrovirus-like sequence (VL30) RNA during

- mouse epidermal cell carcinogenesis. *Mol. Carcinog.* **3**:75–82.
19. Hupp, T. R., D. W. Meek, C. A. Midgley, and D. P. Lane. 1992. Regulation of the specific DNA binding function of p53. *Cell* **71**:875–886.
 20. Kastan, M. B., O. Onyekwere, D. Sidransky, B. Vogelstein, and R. W. Craig. 1991. Participation of p53 protein in the cellular response to DNA damage. *Cancer Res.* **51**:6304–6311.
 21. Kastan, M. B., Q. Zhan, W. S. El-Deiry, F. Carrier, T. Jacks, W. V. Walsh, B. S. Plunkett, B. Vogelstein, and A. Fornace, Jr. 1992. A mammalian cell cycle checkpoint pathway utilizing p53 and *GADD45* is defective in ataxia-telangiectasia. *Cell* **71**:587–597.
 - 21a. Kulesz-Martin, M. Unpublished data.
 22. Kulesz-Martin, M., L. Blumenson, K. F. Manly, J. Siracky, and C. J. East. 1991. Tumor progression of murine epidermal cells after treatment *in vitro* with 12-O-tetradecanoylphorbol-13-acetate or retinoic acid. *Cancer Res.* **51**:4701–4706.
 23. Kulesz-Martin, M., A. E. Kilkenny, K. A. Holbrook, V. Digernes, and S. H. Yuspa. 1983. Properties of carcinogen altered mouse epidermal cells resistant to calcium-induced terminal differentiation. *Carcinog.* **4**:1367–1377.
 24. Kulesz-Martin, M., P. Kozlowski, I. Glurich, B. Lisafeld, E. Hemedinger, and V. Kumar. 1989. Pemphigoid, pemphigus and desmoplakin as antigenic markers of differentiation in normal and tumorigenic mouse keratinocyte lines. *Cell Tissue Kinet.* **22**:279–290.
 25. Kulesz-Martin, M. F., L. Blumenson, and B. Lisafeld. 1986. Retinoic acid enhancement of an early step in the transformation of mouse epidermal cells *in vitro*. *Carcinog.* **7**:1425–1429.
 26. Kulesz-Martin, M. F., M. Yoshida, L. Prestine, S. H. Yuspa, and J. S. Bertram. 1985. Mouse cell clones for improved quantitation of carcinogen-induced altered differentiation. *Carcinog.* **6**:1245–1254.
 27. Lane, D. P. 1992. p53, guardian of the genome. *Nature (London)* **358**:15–16.
 - 27a. Liu, Y., Y. Wu, and M. Kulesz-Martin. Unpublished data.
 28. Milne, D. M., R. H. Palmer, and D. W. Meek. 1992. Mutation of the casein kinase II phosphorylation site abolishes the anti-proliferative activity of p53. *Nucleic Acids Res.* **20**:5565–5570.
 29. Milner, J. 1984. Different forms of p53 detected by monoclonal antibodies in non-dividing and dividing lymphocytes. *Nature (London)* **20**:143–145.
 30. Milner, J. 1991. The role of p53 in the normal control of cell proliferation. *Curr. Opin. Cell Biol.* **3**:282–286.
 31. Milner, J., and E. A. Medcalf. 1991. Cotranslation of activated mutant p53 with wild type drives the wild-type p53 protein into the mutant conformation. *Cell* **65**:765–774.
 32. Momand, J., G. P. Zambetti, D. C. Olson, D. George, and A. J. Levine. 1992. The *mdm-2* oncogene product forms a complex with the p53 protein and inhibits p53-mediated transactivation. *Cell* **69**:1237–1245.
 33. Nigro, J. M., R. Sikorski, S. I. Reed, and B. Vogelstein. 1992. Human p53 and *CDC2Hs* genes combine to inhibit the proliferation of *Saccharomyces cerevisiae*. *Mol. Cell. Biol.* **12**:1357–1365.
 34. Oren, M., and A. J. Levine. 1983. Molecular cloning of a cDNA specific for the murine p53 cellular tumor antigen. *Proc. Natl. Acad. Sci. USA* **80**:56–59.
 35. Prives, C., and J. J. Manfredi. 1993. The p53 tumor suppressor protein: meeting review. *Genes Dev.* **7**:529–534.
 36. Ro, Y. S., P. N. Cooper, J. A. Lee, A. G. Quinn, D. Harrison, D. Lane, C. H. W. Horne, J. L. Rees, and B. Angus. 1993. p53 protein expression in benign and malignant skin tumours. *Br. J. Dermatol.* **12**:237–241.
 37. Ruggeri, B., J. Caamano, T. Goodrow, M. DiRado, A. Bianchi, D. Trono, C. J. Conti, and J. P. Klein-Szanto. 1991. Alterations of the p53 tumor suppressor gene during mouse skin tumor progression. *Cancer Res.* **51**:6615–6621.
 38. Schneider, B. L., G. T. Bowden, C. Sutter, J. Schweizer, K.-A. Han, and M. Kulesz-Martin. 1993. 7,12-Dimethylbenz[α]anthracene-induced mouse keratinocyte transformation without Harvey *ras* protooncogene mutations. *J. Invest. Dermatol.* **101**:595–599.
 39. Seto, E., A. Usheva, G. P. Zambetti, J. Momand, N. Horikoshi, R. Weinmann, A. J. Levine, and T. Shenk. 1992. Wild-type p53 binds to the TATA-binding protein and represses transcription. *Proc. Natl. Acad. Sci. USA* **89**:12028–12032.
 40. Soussi, T., C. Caron deFromentel, and P. May. 1990. Structural aspects of the p53 protein in relation to gene evolution. *Oncogene* **5**:945–952.
 41. Stenger, J. E., G. A. Mayr, K. Mann, and P. Tegtmeyer. 1992. Formation of stable p53 homotetramers and multiples of tetramers. *Mol. Carcinog.* **5**:102–106.
 42. Stephen, C. W., and D. P. Lane. 1992. Mutant conformation of p53. Precise epitope mapping using a filamentous phage epitope library. *J. Mol. Biol.* **225**:577–583.
 43. Sturzbecher, H. S., R. Brain, C. Addison, K. Rudge, M. Remm, M. Grimaldi, E. Keenan, and J. R. Jenkins. 1992. A C-terminal α -helix plus basic region motif is the major structural determinant of p53 tetramerization. *Oncogene* **7**:1513–1523.
 44. Vogelstein, B. 1990. A deadly inheritance. *Nature (London)* **348**:681–682.
 45. Vogelstein, B., and K. W. Kinzler. 1992. p53 function and dysfunction. *Cell* **70**:523–526.
 46. Wade-Evans, A., and J. R. Jenkins. 1985. Precise epitope mapping of the murine transformation-associated protein, p53. *EMBO J.* **4**:699–706.
 47. Weintraub, H., S. Hauschka, and S. J. Tapscott. 1991. The MCK enhancer contains a p53 responsive element. *Proc. Natl. Acad. Sci. USA* **88**:4570–4571.
 48. Wolf, D., N. Harris, N. Goldfinger, and V. Rotter. 1985. Isolation of a full-length mouse cDNA clone coding for an immunologically distinct p53 molecule. *Mol. Cell. Biol.* **5**:127–132.
 49. Wolf, D., N. Harris, and V. Rotter. 1984. Reconstitution of p53 expression in a nonproducer Ab-MuLV-transformed cell line by transfection of a functional p53 gene. *Cell* **38**:119–126.
 50. Yewdell, J. W., J. V. Gannon, and D. P. Lane. 1986. Monoclonal antibody analysis of p53 expression in normal and transformed cells. *J. Virol.* **59**:444–452.
 51. Yonish-Rouach, E., D. Grunwald, S. Wilder, A. Kimchi, E. May, J.-J. Lawrence, P. May, and M. Oren. 1993. p53-mediated cell death: relationship to cell cycle control. *Mol. Cell. Biol.* **13**:1415–1423.
 52. Yonish-Rouach, E., D. Resnitzky, J. Lotem, D. Michael, L. Sachs, A. Kimchi, and M. Oren. 1992. Induction of apoptosis (programmed cell death) by wild-type p53, p. 201–211. *In* D. M. Livingston and E. M. Mihich (ed.), *Tumor suppressor genes*. Pezcoller Foundation Symposium 3. Edigraf, s.r.l., Rome.
 53. Zambetti, G. P., J. Bargonetti, K. Walker, C. Prives, and A. J. Levine. 1992. Wild-type p53 mediates positive regulation of gene expression through a specific DNA sequence element. *Genes Dev.* **6**:1143–1152.